RSC Advances

This article can be cited before page numbers have been issued, to do this please use: H. Andleeb, Y. Tehseen, S. J. A. Shah, I. Khan, J. Iqbal and S. HAMEED, *RSC Adv.*, 2016, DOI: 10.1039/C6RA14531K.

ROYAL SOCIETY OF CHEMISTRY

www.rsc.org/advances

View Article Online
DOI: 10.1039/C6RA14531K

RSC Advances

ARTICLE

Received 00th January 2016,
Accepted 00th January 20xx

DOI: 10.1039/x0xx00000x

www.rsc.org/

Identification of novel pyrazole–rhodanine hybrid scaffolds as potent inhibitors of aldose reductase: design, synthesis, biological evaluation and molecular docking analysis

Hina Andleeb,[a] Yildiz Tehseen,[b] Syed Jawad Ali Shah,[b] Imtiaz Khan,[a] Jamshed Iqbal[b]* and Shahid Hameed[a]*

In an effort to develop a new class of potent aldose reductase inhibitors, a series of 1,3-diarylpyrazole assimilated 3-substituted 4-oxo-2-thioxo-1,3-thiazolidines (**9a–n**) was designed, and synthesized in good to excellent yields by pharmacophore integration approach. The structures of the newly synthesized pyrazole-rhodanine derivatives were established by readily available spectroscopic methods (FTIR, ^{1}H and ^{13}C NMR) and mass spectrometry. The hybrid compounds were evaluated as aldehyde and aldose reductase inhibitors. The biological screening results identified several compounds as remarkable inhibitors of ALR1 and ALR2. Among them, compounds **9c** and **9k** showed excellent activity (and complete selectivity) towards aldose reductase enzyme with IC_{50} values of 1.22 ± 0.67, and 2.34 ± 0.78 µM, respectively, as compared to the standard drug (Sorbinil; IC_{50} = 3.10 ± 0.20 µM). The molecular docking analysis of the most potent inhibitor **9c** was performed in order to identify the putative binding modes inside the active pocket of the enzymes. These newly discovered aldose reductase inhibitors are believed to represent valuable lead structures to further streamline the generation of candidate compounds to target a number of pathological conditions, most strikingly long-term diabetic complications.

Introduction

Aldose reductase (AR) has been implicated in the etiology of diabetic complications that may be attributed to a significant flux of glucose through the polyol pathway, induced in tissues such as nerves, retina, lens and kidney at elevated blood glucose levels. Diabetes, a complex and chronic metabolic disorder, is now recognized as a public health problem. According to epidemiological data, 366 million people were diagnosed with diabetes in 2011, and this number is expected to rise sharply to 552 million people within the next 20 years.[1–3] The economic cost attributable to the management of this disease markedly influences countries' health budgets, being the highest of any disease category.[4,5] Hence, the inhibition of aldose reductase is emerging as a major therapeutic strategy for the treatment of hyperglycemia-induced cardiovascular pathologies.[6] Progression of chronic diabetes results in long-term, debilitating complications such as cataractogenesis and microangiopathy (including nephropathy, retinopathy and neuropathy) thought to be linked to excess free glucose in corresponding tissues.[7,8] Numerous observations have provided evidence of aldose reductase (AR) implication in diabetic complications.[9,10] Inhibition of aldose reductase, the first enzyme of the polyol pathway, is therefore a useful strategy for prevention and treatment of complications of chronic diabetes. A considerable effort in this direction has led to the discovery of a large number of AR inhibitors.[11–14]

Aldose reductase (ALR2; EC 1.1.1.21) is the first rate-determining enzyme in the polyol pathway and catalyses the reduction of glucose to sorbitol with concomitant conversion of NADPH into $NADP^+$ (Fig. 1). Sorbitol is in turn converted into fructose with accompanied reduction of NAD^+ by sorbitol dehydrogenase.[15] Under normal circumstances, glucose is predominantly converted to glucose-6-phosphate by hexokinase and then enters the glycolytic pathway, whereas only a small amount of glucose is metabolized through the polyol pathway due to a relatively low affinity of ALR2 for this substrate. During hyperglycemia, the polyol metabolic pathway is activated and the increased flux of glucose through the polyol pathway triggers the accumulation of sorbitol, which mainly happens in tissues demonstrating insulin-independent uptake of glucose, such as lens, kidney, retina, and peripheral nerves.[16] Because of the excess sugar alcohol (polyol), the lens imbibes water, causing osmotic imbalance. Eventually, increased sodium and decreased potassium levels and decreased glutathione levels lead to cataract formation. Topical administration of aldose reductase inhibitors has been shown to prevent the cataract in rats.[17]

Fig. 1. Polyol pathway for glucose metabolism.

[a] Department of Chemistry, Quaid-i-Azam University, Islamabad-45320, Pakistan. Email: shameed@qau.edu.pk; Fax: +92-51-9064-2241; Tel: +92-51-9064-2133
[b] Centre for Advanced Drug Research, COMSATS Institute of Information Technology, Abbottabad-22060, Pakistan. E-mail: drjamshed@ciit.net.pk; Fax: +92-992-383441; Tel: +92-992-383591, 92-992-383596

Electronic Supplementary Information (ESI) available: [^{1}H NMR, ^{13}C NMR and Mass spectra of all the synthesized compounds]. See DOI: 10.1039/x0xx00000x

View Article Online
DOI: 10.1039/C6RA14531K

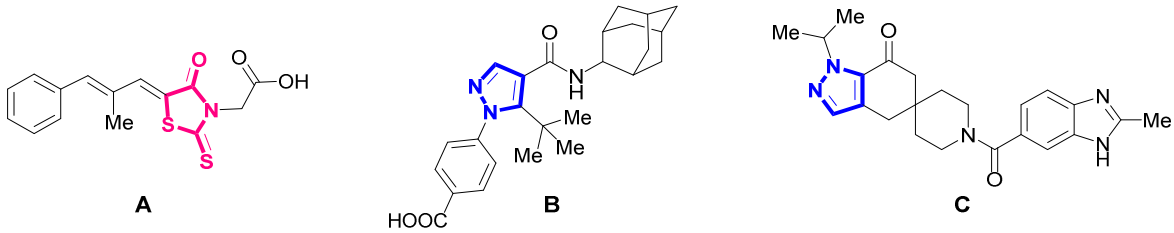

Fig.2. Representative examples of aldose reductase inhibitor (epalrestat; **A**) and pyrazole-based antidiabetic agents (**B** and **C**).

According to recent reports, AR is up-regulated not only under hyperglycemic conditions but also in other pathological states including cardiac disorders (myocardial ischemia and ischemia-reperfusion injury, congestive heart failure, cardiac hypertrophy and cardiomyopathy), inflammation, mood disorders, renal insufficiency, ovarian abnormalities and human cancers such as liver, breast, ovarian, cervical and rectal cancers.[5,18–20] These pathological processes have become major threats to human health in the 21st century. Intense efforts have been directed toward the development of effective aldose reductase inhibitors,[21] however, only a few compounds have reached clinical trials, mostly thiazolidine-2,4-diones such as glitazones (ciglitazone, troglitazone, pioglitazone and rosiglitazone).[22–26] So far, a 2-thioxothazolidine-4-one, epalrestat (Kinedak),[27,28] marketed in Japan and China, is the only commercially available ARI drug. Apart from epalrestat, AR inhibitors have failed in clinical trials because of poor pharmacokinetic properties and side effects,[29] and even epalrestat has been withdrawn from the market in some countries because of its side effects. Thus, it is important to develop novel ARIs with improved efficacy and less toxic profile.

Pyrazoles, key structural fragments in drug discovery, occupy a significant position in medicinal chemistry due to their diverse spectrum of biological activities including anti-viral, antitumor,[30–32] anti-inflammatory,[33] antihyperglycemic,[34,35] and antidiabetic activities.[36–41] Inspired by these findings, and in a continuation of our research interests for the development of novel and effective antidiabetic agents,[42a,b] we focused our attention on the heterocyclic core of epalrestat, (thioxothiazolidine) and pyrazole, exploited previously for numerous pharmacological properties. Idea was to couple the two bioactive nuclei (thioxothiazolidine and pyrazole) using a hybrid pharmacophore approach to develop a novel scaffold with favorable chemical modifications and enhanced aldose reductase inhibitory activities, which to the best of our knowledge, has not been reported previously (Fig. 3). Prompted by this speculation, we embarked on the synthesis of target pyrazole-rhodanine hybrid compounds with structural variations on the aromatic moiety and determined their AR inhibitory potency using an *in vitro* biological assay. The molecular docking investigations provided the insights on the putative binding mode of the potent inhibitor inside the active site of ALR1 and ALR2.

Results and discussion

Chemistry

Synthesis of intermediate pharmacophores **4a–b** and **8a–g** for the formation of target compounds **9a–n** was accomplished according to the synthetic routes illustrated in Schemes 1 and 2. Synthesis was performed using modified literature procedure.[43a-d,44] 3-Bromoaniline/*p*-toluidine (**1**) (1.0 equiv) was reacted with carbon disulfide (2.0 equiv) in diethyl ether in the presence of triethylamine (2.0 equiv) as a base to furnish triethylammonium *N*-aryl dithiocarbamate (**2**), which on subsequent reaction with sodium chloroacetate in ethanol/water (1:1) afforded sodium 2-(*N*-4-substituted phenylcarbamothioylthio)acetate (**3**). The 3-aryl-2-thioxo-1,3-thiazolidin-4-ones (**4a** and **4b**) were synthesized in up to 85% yield by the cyclization of **3** in boiling hydrochloric acid.

One of the most important feature of this synthetic route is the use of 3-(4-substituted phenyl)-1-phenyl-1*H*-pyrazole-4-carbaldehyde as a key starting material for further transformation. The Vilsmeier–Haack cyclization of hydrazones provided an efficient route for the preparation of 1*H*-pyrazole-4-carbaldehydes. Compounds (**8a–g**) were prepared in two steps. In the first step, substituted acetophenones (**6**) and phenyl hydrazine (**5**) were reacted in the presence of glacial acetic acid in ethanol to afford the hydrazone derivative (**7**). The treatment of hydrazone (**7**) under Vilsmeier–Haack (DMF–$POCl_3$) conditions in the second step furnished corresponding 4-carboxaldehyde functionalized pyrazole derivatives (**8a–g**).[45]

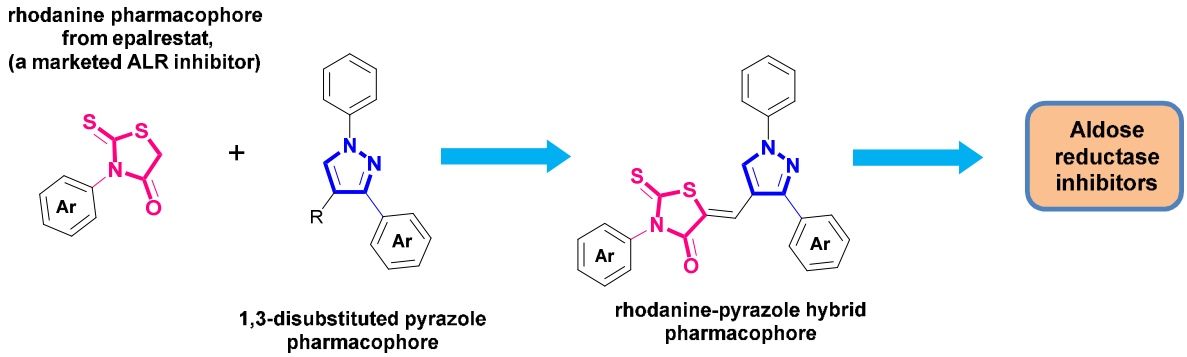

Fig. 3. Structural design of pyrazole-thioxothiazolidine hybrid compounds by pharmacophore integration approach.

View Article Online
DOI: 10.1039/C6RA14531K

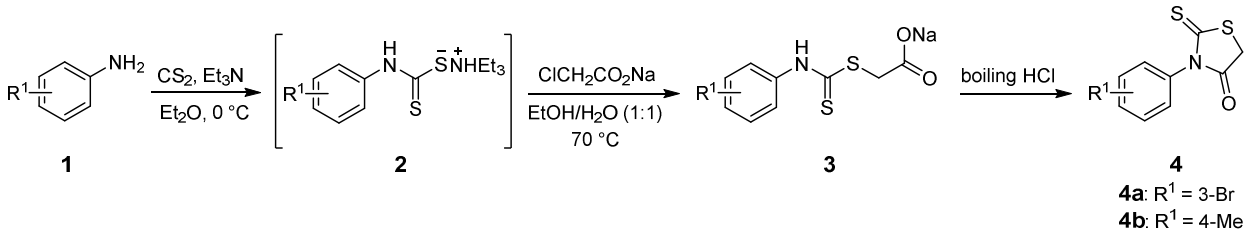

Scheme 1. Synthetic pathway to 3-aryl-2-thioxo-1,3-thiazolidin-4-ones.

The reaction was carried out at 0–70 °C for 3 h using 3 equivalents of the Vilsmeier–Haack reagent, followed by treatment with base ($NaHCO_{3aq}$) affording a series of 3-aryl-1*H*-pyrazole-4-carbaldehydes (**8a-g**) in good yields (Scheme 2).

The pyrazole-rhodanine hybrid compounds 3-(4-substituted phenyl)-5-((1-phenyl-3-aryl-1*H*-pyrazol-4-yl)methylene)-2-thioxothiazolidin-4-ones (**9a–n**) were synthesized by the Knoevenagel condensation of 3-(4-sustituted phenyl)-2-thioxothiazolidin-4-ones (**4a** and **4b**) with 1-phenyl-3-(aryl)-1*H*-pyrazole-4-carbaldehydes (**8a–g**).

The feasibility of the condensation reaction was initially examined using rhodanine (**4a**) and pyrazole-4-carbaldehyde (**8a**) as model substrates (Table 1). The reaction was conducted using acetic acid as a solvent and NaOAc (1.0 equiv) as a base, leading to the desired product **9a** in 40% yield (entry 1). Other solvents such as toluene and water in combination with bases (NH_4OAc and TBAB) gave inferior results (entries 2 and 3). The change of solvent to methanol with the addition of crystalline EDDA as a base produced compound **9a** in 49% yield (entry 4). Notably, EDDA prepared *in situ* (from EDA and AcOH) remained a very appropriate base for this condensation reaction. It was observed that a maximum yield of 81% was achieved using chloroform/ethanol as a solvent at room temperature (entry 5). However, the change of solvent to 1,4-dioxane gave **9a** in 70% yield only (entry 6).

The scope of the Knoevenagel condensation reaction for the preparation of a library of pyrazole-rhodanine hybrid compounds was then explored under the optimized reaction conditions (Table 2). With both the electron-rich and electron-poor substituents on the aryl rings attached to rhodanine and pyrazole cores, the reaction proceeded smoothly and provided the corresponding hybrid compounds (**9a–n**) in good to excellent yields. Gratifyingly, functional groups such as methoxy, methyl, nitro, fluoro, bromo, and hydroxyl were very compatible in the present reaction conditions. Some of the functional groups (halogen & hydroxyl) offer the opportunity for further functionalization to construct more complex molecules.

All the synthesized compounds were characterized by readily available analytical methods including FT-IR, ^1H and ^{13}C NMR spectroscopy and mass spectrometry. In the IR spectra, the stretching vibrations observed around 1600–1560 and 1350–1320 cm^{-1} were attributed to C=N (pyrazole) and C=S functionalities, respectively. The strong bands for carbonyl stretching frequencies appeared in the region 1710–1698 cm^{-1}.

In ^1H NMR spectra, the most characteristic =C–H in the pyrazole ring resonated in the range 8.15-8.88 ppm. The olefinic proton (=C–H) appeared in rather deshielded region of 7.66–7.88 ppm confirming the presence of *Z*-configuration for the exocyclic double bond as is evident from literature[45a-e]. The reason for this deshielding is attributed to the *cis* position of the carbonyl oxygen of rhodanine ring to the =CH hydrogen, and hence *Z* configuration owing to the high degree of thermodynamic stability credited to intramolecular hydrogen bond that can be formed between the hydrogen atom of =CH group and the oxygen atom in rhodanine carbonyl.[45a] ^{13}C NMR spectra showed diagnostic chemical shifts around 193.97–190.54 ppm due to the presence of C=S in the rhodanine ring, whereas, the C=O (rhodanine ring) and C=N (pyrazole ring) functional groups resonated in the regions 167.12–165.63 and 155.63–153.96 ppm, respectively. Finally, the high resolution mass spectra further confirmed the formation of the target compounds **9a–n**.

Enzyme inhibition studies

All of the designed compounds (**9a–n**) were tested for their potential inhibition against aldehyde and aldose reductase enzymes. The isozymes ALR1 and ALR2 belong to the aldo-keto reductases superfamily of enzymes and thus share almost 65% similarity on structure as well as sequence homology. As these are related closely, unwanted effects can be seen with parallel inhibition as ALR1 is normally involved in detoxification of toxic aldehydes.[46] The main objective of the study was to identify most potent and selective inhibitors of ALR1 and ALR2 with an aim to control long-term diabetic complications using the novel synthesized rhodanine derivatives (**9a–n**). The inhibitory response of the synthesized compounds was tested at various concentrations against aldose reductase and produced significant inhibition. The percentage inhibition of each tested compound was calculated and IC_{50} ± SEM (μM) values of most potent compounds were determined using graph pad prism. The inhibition data of the tested series (**9a–n**) is presented in Table 3.

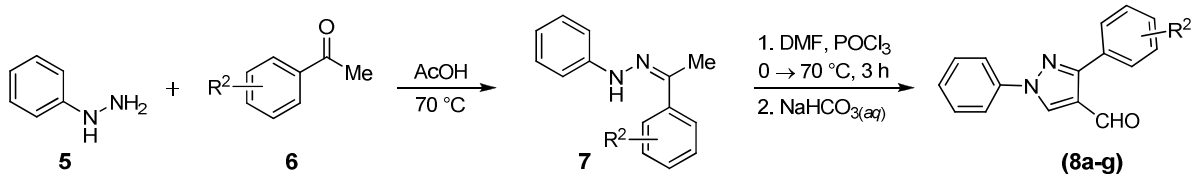

R^2 = H, 4-OMe, 4-Me, 4-NO_2, 4-F, 4-Br, 2-OH

Scheme 2. Synthetic pathway to 1,3-diaryl-1*H*-pyrazole-4-carbaldehyde derivatives (**8a-g**).

View Article Online
DOI: 10.1039/C6RA14531K

Table 1. Optimization of reaction conditions for the synthesis of **9a**.[a]

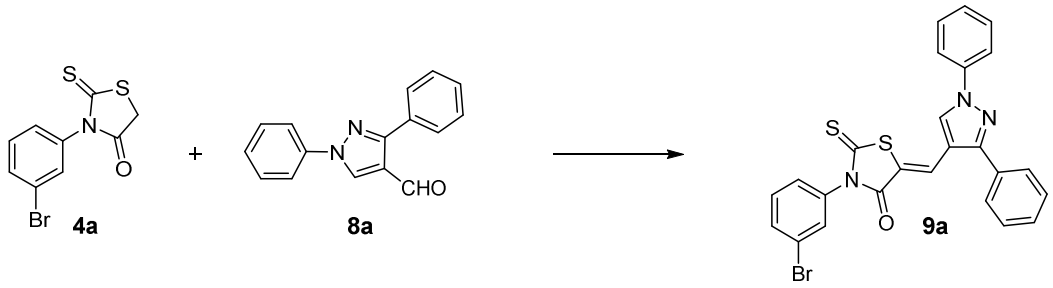

Entry	Solvent	Base (mmol)	T (°C)	Time (h)	Yield (%)[b]
1	AcOH	NaOAc (1.0 mmol)	120	24	40
2	PhMe	NH_4OAc (1.0 mmol)	110	48	10
3	H_2O	TBAB (1.0 mmol)	100	36	13
4	MeOH	EDDA (1.0 mmol)	65	3	49
5	$CHCl_3$:MeOH (8:1)	EDA (0.2 mmol) in AcOH (2 mmol)	25	1	81
6	1,4-dioxane	EDA (0.2 mmol) in AcOH (2 mmol)	25	3	70

[a]The reactions were conducted using **4a** (1.0 mmol) and **8a** (1.2 mmol). [b]Isolated yield. TBAB = Tetrabutylammonium bromide; EDDA = Ethylenediammonium diacetate; EDA = Ethylenediamine.

Among the evaluated compounds, the order showing the highest potency of inhibition was **9h** > **9m** > **9a** > **9n** > **9e** > **9f** against ALR1 while the inhibition potency pattern against ALR2 was **9c** > **9k** > **9i** > **9e** > **9m** > **9h** > **9f** > **9b**. Table 3 clearly demonstrated that the compounds **9a**, **9e**, **9h**, **9m** and **9n** possess better activity as compared to the standard inhibitor (valproic acid) against ALR1 while compounds **9c** and **9k** show potent activity as compared to the standard inhibitor (sorbinil) against ALR2.

The structure-activity relationship analysis of the tested 3-substituted (1,3-diaryl pyrazol-5-yl) methylene rhodanine derivatives revealed that the selectivity and inhibitory activity profile was dependent on the functional groups attached at various positions of the aromatic ring. For example, compound **9h** showed the highest potency against ALR1 with an IC_{50} value of 1.72 ± 0.08 µM, thus approximately 30-fold stronger inhibition as compared to the standard inhibitor (valproic acid; IC_{50} = 57.4 ± 10 µM), while compound **9c** showed highest potency against ALR2 with an IC_{50} value of 1.22 ± 0.67 µM, more than 2-fold stronger inhibition as compared to the standard inhibitor (sorbinil; IC_{50} = 3.10 ± 0.20 µM). Compound **9h** being the most potent towards ALR1 incorporates methyl group at the *para*-position of the aryl ring attached to the rhodanine skeleton and an unsubstituted phenyl ring attached to the pyrazole core. Compound **9h** also demonstrates more selectivity towards ALR1 as compared to ALR2. Introduction of an electron-withdrawing halo group on the phenyl ring of pyrazole produced compound **9m** which is approximately 25-fold stronger inhibitor than valproic acid. The replacement of the methyl group (rhodanine ring) with an electron-withdrawing bromo group at *meta*-position reduces the inhibitory efficacy but, still this affect is ~20-fold higher than the standard inhibitor. Thus, it can be concluded from the results that both electron-rich and electron-poor groups at the aryl rings are essential for the recognition of the enzyme pocket to show the inhibition potential. The structure-activity relationship also illustrated that the presence of functional groups like methoxy, nitro, fluoro (in some cases) at the *para*-position of the aryl ring attached to the pyrazole moiety resulted in reduced inhibition of ALR1, whereas when these groups were replaced with bromo and hydroxyl functionalities, the results demonstrated higher inhibitory potency towards ALR1.

In case of ALR2 inhibition, the lead compound **9c** features a combination of electron-withdrawing (bromo) group at the *meta*-position of the aryl ring (attached to rhodanine) and mild electron-donating (methyl) group at the *para*-position of the aryl ring linked to the pyrazole core. The replacement of bromo group in **9c** with a methyl substituent and methyl group with a more polarized nitro substituent furnished compound **9k** which is also a potent inhibitor with an IC_{50} value of 2.34 ± 0.78 µM. Furthermore, compounds **9c** and **9k** were also identified as selective inhibitors of ALR2. The aryl rings substituted only with electron-rich (methyl and methoxy) groups resulted in compound **9i** which shows significant inhibitory effect with an IC_{50} value of 4.24 ± 1.32 µM. In general, the present study explored a new class of aldose reductase inhibitors based on pyrazole–rhodanine compounds.

Molecular Docking

Molecular docking study of compound **9c** (*z*-isomer) was carried out using FlexX docking utility of LeadIT from BioSolveIT GmbH, Germany.[48] As evident from the *in-vitro* results, the compound **9c** shows more potent inhibition of aldose reductase (ALR2) as compared to aldehyde reductase (ALR1). To understand the molecular basis of such difference in activity, the molecular docking study of the compound is carried out against both enzyme systems.

To perform molecular docking study, the parameters were optimized after successfully reproducing the co-crystallized reference ligand poses with root mean square deviation of 1.890 and 0.695 Å inside ALR1 and ALR2, respectively.

View Article Online
DOI: 10.1039/C6RA14531K

Table 2. Scope of Knoevenagel condensation for the synthesis of pyrazole–rhodanine hybrids (**9a–n**).

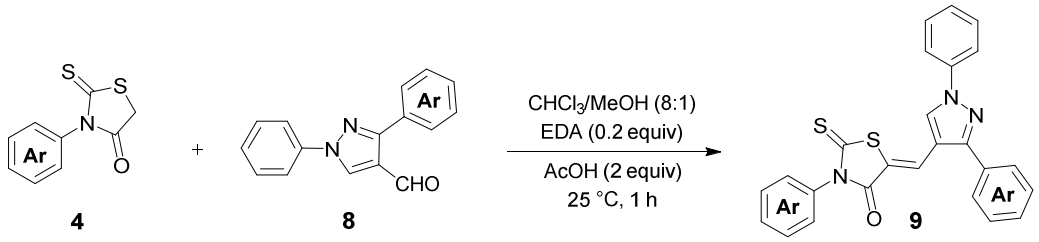

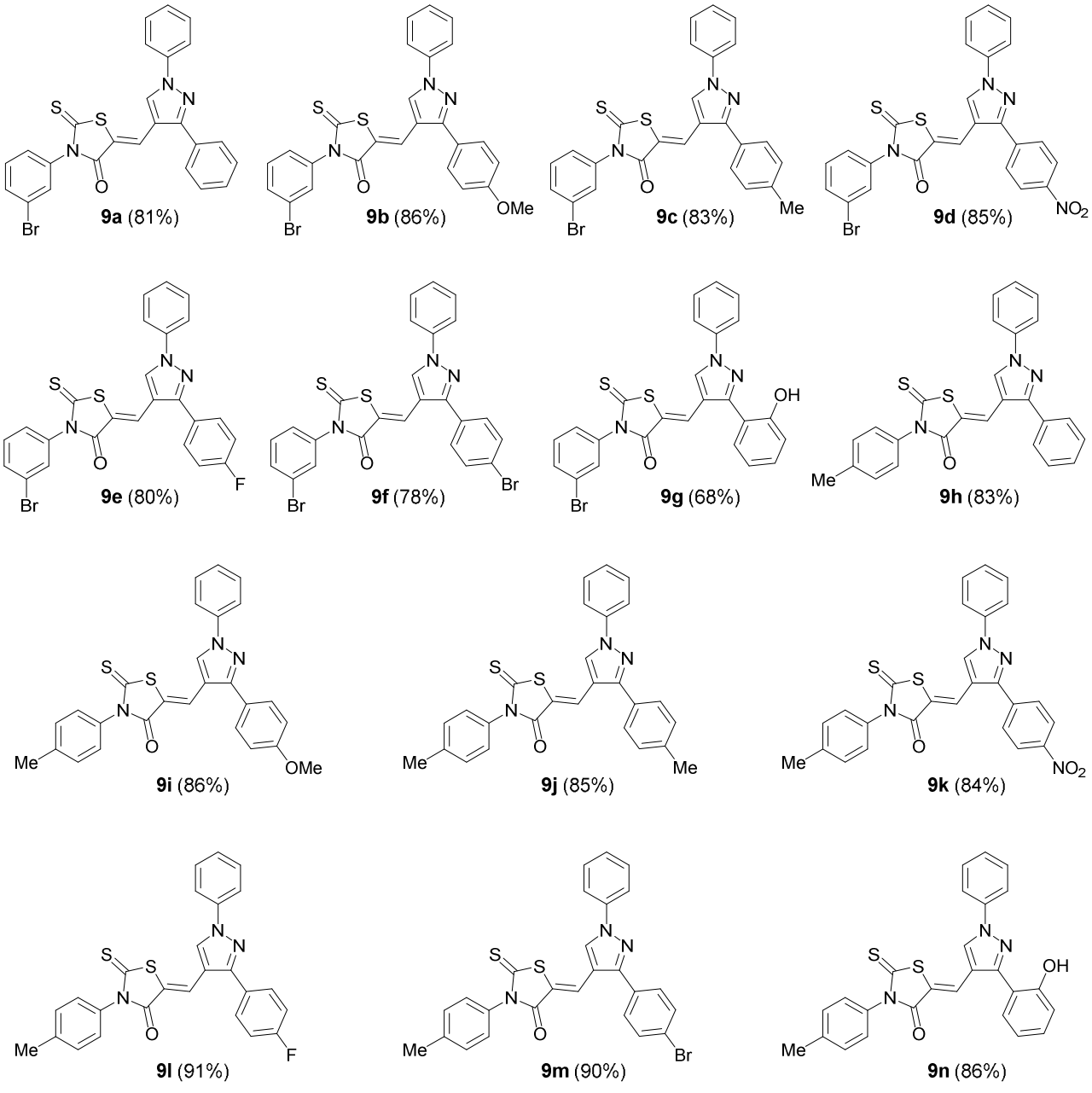

View Article Online
DOI: 10.1039/C6RA14531K

Table 3. Inhibitory efficacy of pyrazole–rhodanine hybrids (**9a–n**) against aldehyde and aldose reductase enzymes.

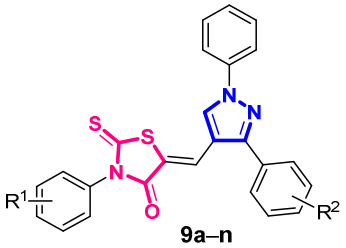

9a–n

Compound	R^1	R^2	ALR1	ALR2
			IC_{50} ± SEM (μM)/%inhibition	
9a	3-Br	H	2.93 ± 0.77	19.76%
9b	3-Br	4-OMe	12.93%	22.68 ± 3.27
9c	3-Br	4-Me	39.38%	1.22 ± 0.67
9d	3-Br	4-NO_2	16.45%	38.52%
9e	3-Br	4-F	22.03 ± 2.11	5.56 ± 1.66
9f	3-Br	4-Br	66.13 ± 5.67	8.08 ± 2.69
9g	3-Br	2-OH	40.92%	42.67%
9h	4-Me	H	1.72 ± 0.08	7.54 ± 2.67
9i	4-Me	4-OMe	11.07%	4.24 ± 1.32
9j	4-Me	4-Me	15.93%	32.55%
9k	4-Me	4-NO_2	21.23%	2.34 ± 0.78
9l	4-Me	4-F	7.07%	46.12%
9m	4-Me	4-Br	2.28 ± 0.70	6.33 ± 2.11
9n	4-Me	2-OH	5.99 ± 1.23	32.93%
Valproic acid	—	—	57.4 ± 10	—
Sorbinil[a]	—	—	—	3.10 ± 0.20

[a]Reported IC_{50} of 3.42 μM of Sorbinil by Rakowitz *et al.*[47a] and Ali *et al.*[47b]

Inside the active pocket of ALR1, the oxygen moiety of thioxothiazolidin-4-one heterocycle ring of compound **9c** forms hydrogen bonding interaction with amino acid Arg309. The compound fails to form any hydrogen bonding interaction with catalytic amino acids His113, previously reported in case of tolrestat and fidarestat[49] which may lead to its poor binding nature and lower binding affinity inside ALR1. Pi–alkyl interactions with amino acid Lys23, Phe125, Ala219 and Pro301 were also observed. The Hyde assessment[50] of compound **9c** inside the ALR1 active site determined maximum binding affinity of –10 $KJmol^{-1}$.

Despite the inability of the compound **9c** to form any hydrogen bonding interactions with previously reported[51] catalytic amino acids such as Tyr48, His110 and Trp111, the compound binds to active pocket of ALR2 with higher binding affinity of –32 $KJmol^{-1}$. The reason for higher binding affinity of the compound **9c** inside ALR2 was determined by Hyde assessment that reveals that the phenyl group attached to the adjacent pyrazole ring of the compound **9c** lies in a perfect alignment inside the specificity pocket formed by amino acids His110, Trp111, Thr113 and Leu300 and thus leading to higher binding affinity.

Large difference in the binding free energy i.e. –32 $KJmol^{-1}$ (inside ALR2) against –10 $KJmol^{-1}$ (inside ALR1) of compound **9c** strongly supports the selectivity determined under *in-vitro* enzyme study. The putative binding mode of the compound **9c** inside ALR1 and ALR2 is illustrated in Fig 4.

OSIRIS drug properties and toxicity profile

The synthesized pyrazole–rhodanine hybrid compounds (**9a–n**) were screened computationally using online OSIRIS property explorer[52] server and were found to possess an average drug score because of their lower water solubility and higher polar surface area. The compounds with –NO_2 substituted groups i.e. **9d** and **9k** were found to show lowest overall drug scores, for compound **9d**, the estimated overall drug score was found to be 0.16 because of its lowest drug likeness of –7.42 while overall drug score of compound **9k** was found to be 0.19 with drug likeness of –5.58. Highest overall drug score was found to be 0.41 for compound **9n** because of the presence of a hydroxyl group with enhanced water

View Article Online
DOI: 10.1039/C6RA14531K

solubility. Details of the OSIRIS drug properties are included in Table 4. When all the synthesized compounds were assessed for drug toxicity on tumorigenic, mutagenic, irritability and reproductive toxicity, they were found non-toxic.

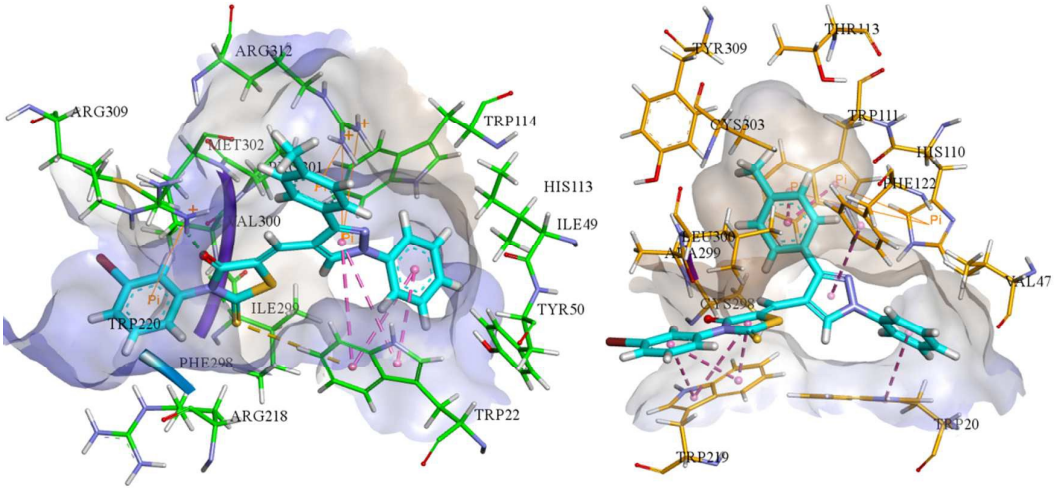

Fig. 4. Putative binding mode of compound **9c** (colored cyan) inside active pocket of ALR1 (colored green) and ALR2 (colored brown). The hydrogen bonding interactions, Pi-Pi interaction and Pi-sulphur interactions are shown in green, pink and yellow colored dashed lines and Pi-charge interaction is shown in solid yellow lines.

Conclusions

In summary, the present study reports successful design and synthesis of a new class of aldose reductase inhibitors based on pyrazole-rhodanine hybrid skeleton. A diverse range of structural variations on the aromatic moiety validated the scope of synthesized derivatives. The designed compounds were tested for their ALR1 and ALR2 inhibitory potency determined through an *in vitro* biological assay using valproic acid and sorbinil as standard inhibitors. Several new compounds demonstrated a strong potential to act as selective and potent inhibitors of both isozymes. Among them, **9a**, **9e**, **9h**, **9m** and **9n** exhibited better activity as compared to the standard inhibitor (valproic acid) against ALR1, while compounds **9c** and **9k** displayed strong inhibitory potential as compared to the standard inhibitor (sorbinil) against ALR2. The structure-activity relationship analysis revealed existence of a delicate balance of attached functional groups to the aryl rings (attached to pyrazole and rhodanine) for potent inhibitory activity, whereas molecular modelling investigations identified the putative binding modes of the lead inhibitors in the active pocket of the enzymes. Hence, the identified inhibitors from the tested series of novel hybrid compounds (**9a–n**) may serve as selective and promising leads for the development of ALR1 and ALR2 inhibitors to treat long term diabetic complications.

Table 4. Drug properties of pyrazole–rhodanine hybrids (**9a–n**) determined by OSIRIS property explorer

Compounds	cLogP	Solubility	Mol. Mass	TPSA	Drug Likeness	Overall Drug Score
9a	4.54	–7.33	517	95.52	2.8	0.31
9b	4.47	–7.35	547	104.7	2.78	0.29
9c	4.88	–7.67	531	95.52	1.28	0.26
9d	3.61	–7.79	562	141.3	–7.42	0.16
9e	4.64	–7.64	535	95.52	2.1	0.28
9f	5.26	–8.16	595	95.52	2.74	0.22
9g	4.19	–7.03	533	115.7	2.35	0.32
9h	4.16	–6.84	453	95.52	4.67	0.39
9i	4.09	–6.86	483	104.7	4.63	0.38
9j	4.50	–7.18	467	95.52	4.46	0.35
9k	3.23	–7.30	498	141.3	–5.58	0.19
9l	4.26	–7.15	471	95.52	3.93	0.36

View Article Online
DOI: 10.1039/C6RA14531K

9m	4.88	–7.67	531	95.52	2.79	0.28
9n	3.81	–6.54	469	115.7	4.24	0.41

Experimental section

Substrates and reagents

The acetophenones and glacial acetic acid were purchased form Sigma-Aldrich (Steinheim, Germany). Anilines and ethylenediamine were the products of Merck (Germany). The reagents used were of analytical grade. Ethanol, chloroform and methanol were supplied by Lab scan (Patuman, Thailand). Dichloromethane and diethyl ether were the products of Riedel de Haen (seezle, Germany) while ethyl acetate and acetone were obtained from commercial sources. All solvents used were either anhydrous or dried.

Instrumentation

All reactions were carried out using oven-dried glassware. Thin layer chromatography (TLC) was performed on Merck precoated $60F_{254}$ (0.2 mm) DF-Aluminium sheets. Compounds were visualized by exposure to UV light at 254 nm. Flash column chromatography was carried out using silica gel (Fisher Scientific 60 Å particle size 35–70 micron). Melting points were recorded in open capillaries using Gallenkamp melting point apparatus (MP-D) and are uncorrected. FTIR spectra were recorded on a Thermoscientific Fourier Transform Infra-Red Spectrophotometer Nicolet 6700 (USA) using Attenuated total refraction (ATR) technique. NMR spectra were acquired on Bruker DQX400 and AV300 spectrometers at room temperature. All chemical shifts are reported in parts per million (ppm). For $CDCl_3$, the shifts are referenced to 7.27 ppm for ^{1}H NMR spectroscopy and 77.0 ppm for ^{13}C NMR spectroscopy. High-resolution mass spectra were recorded on a VG Autospec spectrometer by chemical ionization or on a Micromass LCT electrospray ionization mass spectrometer operating at a resolution of 5000 full width half height. The elemental analysis was performed on Leco CHNS-932 Elemental Analyzer, Leco Corporation (USA).

General procedure for the synthesis of 3-(4-substituted phenyl)-2-thioxo-1,3-thiazolidin-4-ones (4a,b)

To a suspension of aniline (**1**) (0.1 mol) and triethylamine (0.2 mol) in a 250 mL round bottom flask at 0 °C was dropwise added carbon disulfide (0.2 mol) dissolved in diethyl ether (50 mL). The reaction mixture was allowed to stir at the same temperature for 5–6 h. After complete precipitation, the triethylammonium dithiocarbamate (**2**) was filtered *in vacuo* and washed with diethyl ether. The solid product was used in the next step without further purification.

To a stirred solution of sodium chloroacetate (0.1 mol) in H_2O (35 mL) was slowly added a solution of triethylammonium dithiocarbamate (**2**) (0.1 mol) separately dissolved in water/ethanol (1:1) and the resulting mixture was allowed to stir at 70 °C. After completion of the reaction (TLC), the mixture was cooled to room temperature and cautiously poured into boiling hydrochloric acid (12N, 40 mL). After 5 minutes, the solution was allowed to cool slowly to room temperature to precipitate the desired 3-(4-substituted phenyl)-2-thioxo-1,3-thiazolidin-4-one derivatives (**4a,b**). The precipitated solid was filtered and washed with water followed by cold ethanol, dried and recrystallized (ethanol).[44,45] The spectro-analytical data was consistent to that reported in literature.[53,54]

General procedure for the synthesis of phenyl-3-aryl-1*H*-pyrazole-4-carbaldehydes (8a–g)

To a stirred solution of phenyl hydrazine **5** (12 mmol) in absolute ethanol (20 mL) was added an appropriate acetophenone **6** (10 mmol) and glacial acetic acid (0.3 mL). The reaction mixture was stirred at 70 °C. After completion of the reaction (TLC), the excess solvent was evaporated to yield a crude solid which was filtered, washed with cold ethanol, dried and recrystallized (ethanol) to yield the corresponding hydrazone (**7**).

The appropriate acetophenone phenylhydrazone (1.0 mmol) was added to a cold solution of dimethylformamide (4 mL) and phosphorus oxychloride (0.5 g, 3.0 mmol), and the resulting mixture was heated at 70 °C for 3 h. After cooling to room temperature, the reaction mixture was poured into crushed ice, neutralized with an aqueous solution of sodium bicarbonate. The precipitated solid was filtered and purified by flash column chromatography (20% EtOAc in petroleum ether) to afford pyrazole-4-carbaldehydes (**8a–g**).[45] The spectro-analytical data were consistent with those reported in literature.[55–59]

General procedure for the synthesis of 3-aryl-5-((1-phenyl-3-aryl-1*H*-pyrazol-4-yl) methylene)-2-thioxothiazolidin-4-ones (9a–n)

To a stirred solution of 3-(4-substituted phenyl)-2-thioxothiazolidin-4-one (**4a** or **b**) (1.0 mmol) in chloroform/methanol (8:1; 18 mL), glacial acetic acid (2 mmol) was added followed by ethylenediamine (0.2 mmol, 1.1 µL). The resulting mixture was stirred for 15 minutes followed by the addition of an appropriate 1-phenyl-3-(4-substituted phenyl)-1*H*-pyrazole-4-carbaldehyde (**8a–g**) (1.2 mmol) at ambient temperature. After completion of the reaction (TLC; 40% acetone in petroleum ether), the excess solvent was removed to afford a bright yellow solid. The crude solid was washed with water, filtered, dried and recrystallized (chloroform/ethanol) to yield pyrazole-rhodanines (**9a–n**).

(*Z*)-3-(3-Bromophenyl)-5-((1,3-diphenyl-1*H*-pyrazol-4-yl)methylene)-2-thioxothiazolidin-4-one (9a): Yellow solid (81%): m.p 253–256 °C; R_f: 0.72 (30% acetone/*n*-hexane); IR (ATR, cm^{-1}): 3011 (Ar–H), 1727 (C=O), 1612 (C=N), 1568, 1509 (C=C), 1215 (C=S); ^{1}H NMR (400 MHz, $CDCl_3$) δ 8.16 (1H, s, =C-$H_{pyrazole}$), 7.77–7.75 (3H, m, ArH and =C-$H_{olefinic}$), 7.74–7.64 (3H, m, ArH), 7.59–7.49 (6H, m, ArH), 7.47–7.41 (2H, m, ArH), 7.30–7.27 (1H, m, ArH); ^{13}C NMR (100.6 MHz, $CDCl_3$) δ 191.56 (C=S), 166.70 (C=O), 155.25, 139.09, 135.95, 132.90, 131.62, 131.24, 130.70, 129.77, 129.25, 129.00, 127.95, 127.69, 127.28, 124.84, 122.77, 121.11, 119.67, 116.54; HRMS (ESI) Exact mass calculated for $C_{25}H_{17}BrN_3OS_2$ $[M+H]^+$: 517.99909, found: 517.99910. Analysis calcd: C, 57.92; H, 3.11; N, 8.10; S, 12.37. Found: C, 58.01; H, 3.07; N, 8.16; S, 12.43.

(*Z*)-3-(3-Bromophenyl)-5-((3-(4-methoxyphenyl)-1-phenyl-1*H*-pyrazol-4-yl)methylene)-2-thioxothiazolidin-4-one (9b): Yellow solid (86%): m.p 283–286 °C; R_f: 0.71 (30% acetone/*n*-hexane); IR (ATR, cm^{-1}): 3010 (Ar-H), 2938, 2803 (CH_3), 1725 (C=O), 1610 (C=N), 1565, 1502 (C=C), 1218 (C=S); ^{1}H NMR (400 MHz, $CDCl_3$) δ 8.16 (1H, s, =C-$H_{pyrazole}$), 7.82 (2H, m, ArH), 7.66–7.57 (1H, s, =C-$H_{olefinic}$), 7.56–7.51 (2H, m, ArH), 7.48 (1H, t, *J* = 1.9 Hz, ArH), 7.45–7.37 (3H, m, ArH), 7.27 (1H, s, ArH), 7.06–7.02 (2H, m, ArH), 3.74 (3H, s, OCH_3); ^{13}C NMR (100.6 MHz, $CDCl_3$) δ 191.77 (C=S), 166.65 (C=O), 154.95, 153.82, 139.05, 132.17, 131.56, 130.44, 130.36, 129.92, 129.80, 127.97, 127.72, 123.59, 123.47, 123.24, 122.46, 121.10, 119.64, 116.59, 112.45, 55.98 (OCH_3); HRMS (ESI) Exact mass calculated for $C_{26}H_{19}BrN_3O_2S_2$ $[M+H]^+$: 548.00966, found: 548.00964. Analysis

View Article Online
DOI: 10.1039/C6RA14531K

calcd: C, 56.94; H, 3.31; N, 7.66; S, 11.69. Found: C, 55.01; H, 3.35; N, 7.72; S, 11.75.

(*Z*)-3-(3-Bromophenyl)-5-((1-phenyl-3-(*p*-tolyl)-1*H*-pyrazol-4-yl)methylene)-2-thioxothiazolidin-4-one (9c): Yellow solid (83%): m.p 223–226 °C; R_f: 0.69 (30% acetone/*n*-hexane); IR (ATR, cm^{-1}): 3017 (Ar-H), 2948, 2813 (CH_3), 1725 (C=O), 1615 (C=N), 1564, 1502 (C=C), 1214 (C=S); ^{1}H NMR (400 MHz, $CDCl_3$) δ 8.13 (1H, s, =C-$H_{pyrazole}$), 7.73 (3H, m, ArH, =C-$H_{olefinic}$), 7.51 (1H, m, ArH), 7.45 (2H, d, *J* = 7.8 Hz, ArH), 7.46–7.29 (3H, m, ArH), 7.34–7.22 (2H, m, ArH), 7.23–7.09 (3H, m, ArH), 2.35 (3H, s, CH_3); ^{13}C NMR (100.6 MHz, $CDCl_3$) δ 190.54 (C=S), 165.63 (C=O), 154.26, 138.23, 138.04, 134.91, 131.81, 130.57, 129.62, 128.68, 128.65, 127.80, 127.28, 126.80, 126.56, 126.23, 123.99, 121.70, 119.81, 118.57, 115.43, 20.36 (CH_3); HRMS (ESI) Exact mass calculated for $C_{26}H_{19}BrN_3OS_2$ $[M+H]^+$: 532.01474, found: 532.01467. Analysis calcd: C, 58.65; H, 3.41; N, 7.89; S, 12.04. Found: C, 58.69; H, 3.48; N, 7.85; S, 12.00.

(*Z*)-3-(3-Bromophenyl)-5-((3-(4-nitrophenyl)-1-phenyl-1*H*-pyrazol-4-yl)methylene)-2-thioxothiazolidin-4-one (9d): Yellow solid (85%): m.p 282–285 °C; R_f: 0.43 (30% acetone/*n*-hexane); IR (ATR, cm^{-1}): 3009 (Ar-H), 1722 (C=O), 1609 (C=N), 1565, 1512 (C=C), 1213 (C=S); ^{1}H NMR (400 MHz, $CDCl_3$): δ 8.34–8.28 (2H, m, ArH), 8.19 (1H, s, =C-$H_{pyrazole}$), 7.84–7.79 (2H, m, ArH), 7.78–7.73 (2H, m, ArH), 7.70 (1H, s, =C-$H_{olefinic}$), 7.60–7.56 (1H, m, ArH), 7.50 (2H, dd, *J* = 8.6, 7.3 Hz), 7.41–7.34 (3H, m, ArH), 7.21–7.18 (1H, m, ArH); ^{13}C NMR (100.6 MHz, $CDCl_3$): δ 191.00 (C=S), 166.48 (C=O), 152.27, 148.02, 138.73, 137.63, 135.65, 132.93, 131.47, 130.68, 129.81, 129.53, 128.32, 127.98, 127.11, 124.14, 122.87, 122.74, 122.65, 119.67, 116.72; HRMS (ESI) Exact mass calculated for $C_{25}H_{16}BrN_4O_3S_2$ $[M+H]^+$: 562.98417, found: 562.98414. Analysis calcd: C, 53.29; H, 2.68; N, 9.94; S, 11.38. Found: C, 53.35; H, 2.76; N, 9.91; S, 11.42.

(*Z*)-3-(3-Bromophenyl)-5-((3-(4-fluorophenyl)-1-phenyl-1*H*-pyrazol-4-yl)methylene)-2-thioxothiazolidin-4-one (9e): Yellow solid (80%): m.p 277–279 °C; R_f: 0.67 (30% acetone/*n*-hexane); IR (ATR, cm^{-1}): 3011 (Ar-H), 1710 (C=O), 1625 (C=N), 1568, 1518 (C=C), 1202 (C=S); ^{1}H NMR (400 MHz, $CDCl_3$): δ 8.15 (1H, s, =C-$H_{pyrazole}$), 7.77–7.72 (2 H, m, ArH), 7.73–7.69 (1H, s, =C-$H_{olefinic}$), 7.62–7.55 (3H, m, ArH), 7.51–7.43 (2H, m, ArH), 7.41–7.31 (3H, m, ArH), 7.21–7.10 (4H, m, ArH); ^{13}C NMR (100.6 MHz, $CDCl_3$): δ 191.43 (C=S), 166.68 (C=O), 164.69, 162.21, 154.23, 139.01, 135.89, 132.94, 131.60, 130.84, 130.75, 130.72, 129.80, 128.03, 127.71, 127.25, 124.32, 122.79, 119.66, 116.25, 116.03; HRMS (ESI) Exact mass calculated for $C_{25}H_{16}BrFN_3OS_2$ $[M+H]^+$: 535.98967, found: 535.98967. Analysis calcd: C, 55.97; H, 2.82; N, 7.83; S, 11.95. Found: C, 56.03; H, 2.91; N, 7.87; S, 11.99.

(*Z*)-3-(3-Bromophenyl)-5-((3-(4-bromophenyl)-1-phenyl-1*H*-pyrazol-4-yl)methylene)-2-thioxothiazolidin-4-one (9f): Yellow solid (78%): m.p 255–259 °C; R_f: 0.65 (30% acetone/*n*-hexane); IR (ATR, cm^{-1}): 3009 (Ar-H), 1718 (C=O), 1625 (C=N), 1548, 1518 (C=C), 1225 (C=S); ^{1}H NMR (400 MHz, $CDCl_3$): δ 8.15 (1H, s, =C-$H_{pyrazole}$), 7.78–7.66 (3H, d, *J* = 7.6Hz, ArH), 7.73 (1H, s, =C-$H_{olefinic}$)7.58 (3H, m, ArH), 7.53–7.43 (4H, m, ArH), 7.43–7.31 (3H, m, ArH), 7.17 (1H, m, ArH); ^{13}C NMR (100.6 MHz, $CDCl_3$): δ 191.38 (C=S), 166.64 (C=O), 153.96, 138.98, 135.87, 132.95, 132.22, 131.60, 130.72, 130.43, 130.22, 129.81, 128.09, 127.79, 127.25, 124.05, 123.72, 122.80, 121.64, 119.68, 116.45; HRMS (ESI) Exact mass calculated for $C_{25}H_{16}Br_2N_3OS_2$ $[M+H]^+$: 595.90961, found: 595.90941. Analysis calcd: C, 50.27; H, 2.53; N, 7.03; S, 10.74. Found: C, 50.33; H, 2.57; N, 7.09; S, 10.79.

(*Z*)-3-(3-Bromophenyl)-5-((3-(2-hydroxyphenyl)-1-phenyl-1*H*-pyrazol-4-yl)methylene)-2-thioxothiazolidin-4-one (9g): Yellow solid (68%): m.p 211–213 °C; R_f: 0.34 (30% acetone/*n*-hexane); IR (ATR, cm^{-1}): 3433 (OH), 3019 (Ar-H), 1735 (C=O), 1613 (C=N), 1560, 1511 (C=C), 1209 (C=S); ^{1}H NMR (400 MHz, $CDCl_3$): δ 8.20 (1H, s, =C-$H_{pyrazole}$), 7.88 (1H, s, =C-$H_{olefinic}$), 7.68 (2H, d, *J* = 7.9 Hz, ArH), 7.65–7.52 (2H, m, ArH, OH), 7.49 (2H, t, *J* = 7.7 Hz, ArH), 7.46–7.41 (2H, m, ArH), 7.38 (2H, dd, *J* = 7.8, 4.3 Hz, ArH), 7.32–7.25 (1H, m, ArH), 7.23–7.19 (1H, m, ArH), 7.06 (1H, d, *J* = 8.2 Hz, ArH), 6.96 (1H, t, *J* = 7.7 Hz, ArH); ^{13}C NMR (100.6 MHz, $CDCl_3$): δ 191.27 (C=S), 166.46 (C=O), 155.63, 152.13, 138.24, 135.72, 132.89, 131.50, 130.88, 130.65, 129.88, 129.00, 128.77, 127.90, 127.15, 124.11, 122.72, 122.53, 120.15, 119.40, 117.38, 116.54, 115.58; HRMS (ESI) Exact mass calculated for $C_{25}H_{17}BrN_3O_2S_2$ $[M+H]^+$: 533.99401, found: 533.99414. Analysis calcd: C, 56.18; H, 3.02; N, 7.86; S, 12.00. Found: C, 56.24; H, 3.08; N, 7.93; S, 12.05.

(*Z*)-5-((1,3-Diphenyl-1*H*-pyrazol-4-yl)methylene)-2-thioxo-3-(*p*-tolyl)thiazolidin-4-one (9h): Yellow solid (83%): m.p 226–229 °C; R_f: 0.76 (30% acetone/*n*-hexane); IR (ATR, cm^{-1}): 3009 (Ar-H), 2943, 2817 (CH_3), 1746 (C=O), 1616 (C=N), 1567, 1509 (C=C), 1219 (C=S); ^{1}H NMR (400 MHz, $CDCl_3$): δ 8.16 (1H, s, =C-$H_{pyrazole}$), 7.79–7.71 (3H, m, ArH, =C-$H_{olefinic}$), 7.66–7.56 (2H, m, ArH), 7.44-7.38 (5H, m, ArH), 7.37–7.27 (1H, m, ArH), 7.26–7.06 (3H, m, ArH), 2.35 (3H, s, CH_3); ^{13}C NMR (100.6 MHz, $CDCl_3$): δ 192.25 (C=S), 167.08 (C=O), 155.15, 139.90, 139.13, 132.20, 131.33, 130.30, 129.75, 129.18, 129.00, 128.99, 128.01, 127.87, 127.65, 124.31, 121.60, 119.65, 116.64, 21.43; HRMS (ESI) Exact mass calculated for $C_{26}H_{20}N_3OS_2$ $[M+H]^+$: 454.10423, found: 454.10407. Analysis calcd: C, 68.85; H, 4.22; N, 9.26; S, 14.14. Found: C, 68.91; H, 4.28; N, 9.29; S, 14.19.

(*Z*)-5-((3-(4-Methoxyphenyl)-1-phenyl-1*H*-pyrazol-4-yl)methylene)-2-thioxo-3-(*p*-tolyl)thiazolidin-4-one (9i): Yellow solid (86%): m.p 243–246 °C; R_f: 0.74 (30% acetone/*n*-hexane); IR (ATR, cm^{-1}): 3012 (Ar-H), 2958, 2823 (CH3), 1716 (C=O), 1609 (C=N), 1563, 1502 (C=C), 1211 (C=S); ^{1}H NMR (300 MHz, $CDCl_3$): δ 8.25 (1H, s, =C-$H_{pyrazole}$), 7.86–7.83 (3H, m, ArH, =C-$H_{olefinic}$), 7.66–7.61 (2H, m, ArH), 7.58–7.53 (2H, m, ArH), 7.44–7.36 (3H, m, ArH), 7.20 (2H, d, *J* = 8.1 Hz, ArH), 3.89 (3H, s, OCH_3), 2.45 (3H, s, CH_3); ^{13}C NMR (75 MHz, $CDCl_3$): δ 192.32 (C=S), 167.12 (C=O), 160.44, 155.02, 139.90, 139.16, 132.31, 130.30, 130.27, 129.74, 128.01, 127.78, 127.57, 124.57, 123.77, 121.28, 119.60, 116.49, 114.46, 55.43 (OCH_3), 21.42 (CH_3); HRMS (ESI) Exact mass calculated for $C_{27}H_{22}N_3O_2S_2$ $[M+H]^+$: 484.11479, found: 484.11459. Analysis calcd: C, 67.06; H, 4.38; N, 8.69; S, 13.26. Found: C, 67.11; H, 4.43; N, 8.74; S, 13.31.

(*Z*)-5-((1-Phenyl-3-(*p*-tolyl)-1*H*-pyrazol-4-yl)methylene)-2-thioxo-3-(*p*-tolyl)thiazolidin-4-one (9j): Yellow solid (85%): m.p 235–239 °C; R_f: 0.71 (30% acetone/*n*-hexane); IR (ATR, cm^{-1}): 3049 (Ar-H), 2968, 2818 (CH_3), 1735 (C=O), 1618 (C=N), 1565, 1512 (C=C), 1208 (C=S); ^{1}H NMR (300 MHz, $CDCl_3$): δ 8.25 (1H, s, =C-$H_{pyrazole}$), 7.86–7.83 (3H, m, ArH, =C-$H_{olefinic}$), 7.61–7.53 (4H, m, ArH), 7.44–7.28 (5H, m, ArH), 7.21–7.18 (2H, m, ArH), 2.45 (6H, s, 2 × CH_3); ^{13}C NMR (75 MHz, $CDCl_3$): δ 192.33 (C=S), 167.09 (C=O), 155.25, 139.90, 139.22, 139.16, 132.31, 131.31, 129.74, 129.69, 128.87, 128.42, 128.02, 127.80, 127.60, 124.55, 121.36, 119.63, 119.49, 116.59, 21.43 (CH_3); HRMS (ESI) Exact mass calculated for $C_{27}H_{22}N_3OS_2$ $[M+H]^+$: 468.11988, found: 468.11968. Analysis calcd: C, 69.35; H, 4.53; N, 8.99; S, 13.71. Found: C, 69.39; H, 4.58; N, 8.94; S, 13.65.

(*Z*)-5-((3-(4-Nitrophenyl)-1-phenyl-1*H*-pyrazol-4-yl)methylene)-2-thioxo-3-(*p*-tolyl)thiazolidin-4-one (9k): Yellow solid (84%): m.p 252–256 °C; R_f: 0.54 (30% acetone/*n*-hexane); IR (ATR, cm^{-1}): 3005 (Ar-H), 2928, 2822 (CH_3), 1703 (C=O), 1617 (C=N), 1555, 1512 (C=C), 1223 (C=S); ^{1}H NMR (300 MHz, $CDCl_3$): δ 8.40 (2H, d, *J* = 6.9 Hz, ArH), 8.29 (1H, s, =C-$H_{pyrazole}$), 7.92 (2H, d, *J* = 6.9 Hz, ArH), 7.85 (2H, d, *J* = 7.5 Hz, ArH), 7.77 (1H, s, =C-$H_{olefinic}$), 7.62–7.56 (2H, m, ArH),

View Article Online
DOI: 10.1039/C6RA14531K

7.49–7.47 (1H, m, ArH), 7.39 (2H, d, *J* = 8.1 Hz, ArH), 7.18 (2H, m, ArH), 2.46 (3H, s, CH_3); ^{13}C NMR (75 MHz, $CDCl_3$): 191.82 (C=S), 166.98 (C=O), 152.28, 148.07, 140.09, 138.87, 137.83, 132.08, 131.28, 130.38, 129.90, 129.62, 128.36, 127.94, 124.23, 123.22, 122.46, 119.74, 116.93, 21.43 (CH_3); HRMS (ESI) Exact mass calculated for $C_{26}H_{19}N_4O_3S_2$ $[M+H]^+$: 499.08931, found: 499.08926. Analysis calcd: C, 62.63; H, 3.64; N, 11.24; S, 12.86. Found: C, 62.67; H, 3.69; N, 11.29; S, 12.82.

(*Z*)-5-((3-(4-Fluorophenyl)-1-phenyl-1*H*-pyrazol-4-yl)methylene)-2-thioxo-3-(*p*-tolyl)thiazolidin-4-one (9l): Yellow solid (91%): m.p 247–250 °C; R_f: 0.64 (30% acetone/*n*-hexane); IR (ATR, cm^{-1}): 3020 (Ar-H), 2918, 2833 (CH_3), 1724 (C=O), 1600 (C=N), 1549, 1512 (C=C), 1219 (C=S); ^{1}H NMR (400 MHz, $CDCl_3$): δ 8.13 (1H, s, =C-$H_{pyrazole}$), 7.75–7.73 (3H, m, ArH, =C-$H_{olefinic}$), 7.51 (1H, m, ArH), 7.45 (2H, d, *J* = 7.8 ArH), 7.46–7.29 (3H, m, ArH), 7.34–7,22 (2H, m, ArH), 7.23–7.16 (3H, m, ArH), 2.35 (3H, s, CH_3); ^{13}C NMR (100.6 MHz, $CDCl_3$): δ 190.54 (C=S), 165.62 (C=O), 154.26, 138.23, 138.04, 134.91, 131.81, 130.57, 129.62, 128.68, 128.65, 127.80, 127.28, 126.80, 126.56, 126.23, 123.99, 121.70, 119.81, 118.57, 115.43, 20.36 (CH_3); HRMS (ESI) Exact mass calculated for $C_{26}H_{19}FN_3OS_2$ $[M+H]^+$: 472.09481, found: 472.09477. Analysis calcd: C, 66.22; H, 3.85; N, 8.91; S, 13.60. Found: C, 66.26; H, 3.89; N, 8.85; S, 13.63.

(*Z*)-5-((3-(4-Bromophenyl)-1-phenyl-1*H*-pyrazol-4-yl)methylene)-2-thioxo-3-(*p*-tolyl)thiazolidin-4-one (9m): Yellow solid (90%): m.p 269–272 °C; R_f: 0.59 (30% acetone/*n*-hexane); IR (ATR, cm^{-1}): 3007 (Ar-H), 2958, 2825 (CH_3), 1728 (C=O), 1677 (C=N), 1564, 1508 (C=C), 1219 (C=S); ^{1}H NMR (300MHz, $CDCl_3$): δ 8.35 (1H, s, =C-$H_{pyrazole}$), 7.82 (2H, m, ArH), 7.77 (1H, s, =C-$H_{olefinic}$), 7.68–7.64 (2H, m, ArH), 7.60–7.53 (4H, m, ArH), 7.46–7.36 (3H, m, ArH), 7.29 (1H, t, *J* = 1.3 Hz, ArH), 7.20–7.17 (2H, m, ArH), 2.46 (3H, s, CH_3); ^{13}C NMR (75 MHz, $CDCl_3$): δ 192.09 (C=S), 167.03 (C=O), 153.87, 139.97, 139.02, 132.20, 130.43, 130.34, 129.80, 128.02, 127.98, 127.76, 123.64, 123.54, 122.12, 119.66, 116.55, 21.43 (CH_3); HRMS (ESI) Exact mass calculated for $C_{26}H_{19}BrN_3OS_2$ $[M+H]^+$: 532.01474, found: 532.01470. Analysis calcd: C, 58.65; H, 3.41; N, 7.89; S, 12.04. Found: C, 58.68; H, 3.46; N, 7.93; S, 12.01.

(*Z*)-5-((3-(2-Hydroxyphenyl)-1-phenyl-1*H*-pyrazol-4-yl)methylene)-2-thioxo-3-(*p*-tolyl)thiazolidin-4-one (9n): Yellow solid (66%): m.p 224–228 °C; R_f: 0.42 (30% acetone/*n*-hexane); IR (ATR, cm^{-1}): 3428 (OH), 3010 (Ar-H), 2948, 2813 (CH_3), 1725 (C=O), 1610 (C=N), 1545, 1512 (C=C), 1219 (C=S); ^{1}H NMR (300 MHz, $CDCl_3$): δ 9.99 (1H, s, OH), 8.88 (1H, s, =C-$H_{pyrazole}$), 7.98–7.92 (2H, m, ArH), 7.68 (1H, s, =C-$H_{olefinic}$), 7.67–7.65 (2H, m, ArH), 7.61–7.52 (7H, m, ArH), 7.46–7.35 (3H, m, ArH), 2.38 (3H, s, CH_3); ^{13}C NMR (75 MHz, $CDCl_3$): δ 193.97 (C=S), 167.12 (C=O), 139.57, 139.15, 135.28, 133.06, 131.59, 130.28, 130.20, 130.09, 129.49, 129.26, 128.88, 128.12, 123.29, 122.61, 122.48, 119.97, 119.70, 119.17, 116.16, 21.29 (CH_3); HRMS (ESI) Exact mass calculated for $C_{26}H_{20}N_3O_2S_2$ $[M+H]^+$: 470.09914, found: 470.09919. Analysis calcd: C, 66.50; H, 4.08; N, 8.95; S, 13.66. Found: C, 66.56; H, 4.13; N, 8.98; S, 13.62.

Enzymatic activity

All chemicals required in the enzyme extraction procedure were of high analytical grade. For measurement of enzymatic reaction ELIZA (Bio-Tek ELx800TM Instrument, Inc. USA) microplate reader of 340 nm UV range and 96 well-plates was used for the sample analysis. Micropipettes from Gilson were used for sample loading. Sodium D-glucoronate and D,L-glyceraldehyde were used as substrates along with a cofactor *i.e.* NADPH (nicotinamide adenine dinucleotide phosphate) from Sigma Aldrich (London, UK).

Isolation and purification of aldehyde reductase (ALR1)

The enzyme aldehyde reductase was extracted from freshly slaughtered bovine kidneys (obtained from the local slaughter house) which were dissected carefully through the cortex area and the dissected tissue was dissolved in 3 times its volume of 10 mM sodium phosphate buffer containing 2.0 mM ETDA dipotassium salt, 2.5 mM β-mercaptoethanol and 0.25 M sucrose at 7.2 pH for homogenization step. The homogenate was then further centrifuged at 12000 rpm for 30 min at 4 °C. The precipitates were discarded to remove the remaining insoluble lipids. It was further processed with 40% ammonium sulphate saturation in order to isolate the required ALR1 enzyme, followed by centrifugation at 12000 rpm for 30 min at 4 °C. The supernatant was again subjected to 50% and 75% ammonium sulphate saturation after removal of the precipitates followed by centrifugation at 12000 rpm for 30 min at 4 °C, thus resulting in the extraction of ALR1 enzyme pellet. The supernatant was discarded and the pellet was redissolved in the second buffer containing sodium phosphate 10 mM at pH 7.2, 2.5 mM β-mercaptoethanol and 2.0 mM ETDA dipotassium salt. The suspension was dialyzed overnight in the dialysis membrane in the same buffer. The solution in the dialysis membrane contained the extracted ALR1 and was aliquoted and stored at –80 °C until used.[60]

Isolation and purification of aldose reductase (ALR2)

The enzyme ALR2 was isolated from the calf lenses removed from the eyes of freshly slaughtered animals in the local slaughter house. Lenses (100–200g) were homogenized in 3 volumes of 10 mM sodium phosphate buffer (pH 7.2), 2.0 mM EDTA dipotassium salt and 2.5 mM β-mercaptoethanol for 20 min. Homogenate was centrifuged at 10,000 rpm for 15 minutes at 4 °C to remove insoluble material. Precipitated material containing lipids was discarded. Supernatant layer was separated and ammonium sulphate salt was added to make the saturation up to 30%. It was centrifuged at 10,000 rpm for 15 min and the precipitate again was discarded. Pure ALR2 was precipitated by addition of powdered ammonium sulfate to 80% saturation. After centrifugation, supernatant was discarded and the precipitated enzyme was redissolved in 50 mM NaCl and dialyzed over night against 4 litres 50 mM NaCl. The volume of the suspension was recorded and the sample was dialyzed overnight against 50 mM NaCl (double replacement of dialysis solution). After dialysis, the volume of the sample was recorded, treated with liquid nitrogen and samples stored in 1 mL aliquots in the eppendorf tubes at –80 °C for the determination of the total protein, enzyme activity and inhibition studies.[60]

Determination of aldose reductase inhibitory activity

UV spectrophotometer was used at 340 nm in order to determine the activity of aldehyde reductase by measuring the NADPH consumption. Each well of the 96-well plate contains exactly 200 µL of assay mixture containing phosphate buffer 100 mM at pH 6.2 with 20 µL of 10 mM test compound followed by addition of 70 µL of enzyme and 40 µL of substrate. The mixture was incubated at 37 °C for 5 min and for the enzymatic reaction to run properly 0.1 mM NADPH (50 µL) as a cofactor was added and reading was taken at 340 nm. The mixture was incubated again at 37 °C for 10 min and reading was taken at the respective UV range in ELIZA plate reader. As positive and negative control, 20 µL of 10 mM valproic acid and buffer solution, respectively, were used.[60] The enzymatic reaction was run in triplicate with a final volume of 200 µL in each well. Absorbance was noted and results were analysed via version 5 GraphPad prism software and IC_{50} values calculated. The total percentage inhibition was calculated by the formula:

View Article Online
DOI: 10.1039/C6RA14531K

$$\%Inhibition = [100 - (Absorbance_{testwell}/Absorbance_{control})] \times 100$$

Molecular Docking

To carry out molecular docking study of compound **9c**, the corresponding structure was drawn using ACD/ChemSketch[61] and was 3D optimized. Crystal structure of porcine aldehyde reductase PDB ID 3FX4 and crystal structure of human aldose reductase PDB ID 1US0 was downloaded from RCSB Protein Databank.[62] Using 'Load or Prepare receptor' utility of LeadIT from BioSolveIT GmbH, Germany, the enzymes crystal structure was loaded and prepared. The co-crystallized cofactor inside the receptor structure was selected as part of the docking study. The cofactor in case of ALR1 was nicotinamide adenine dinucleotide phosphate (NADP), while in case of ALR2, the cofactor was dihydro nicotinamide adenine dinucleotide phosphate (NADPH). Using Protoss[63] utility of the software water handling, protonation state and tautomer state of the active site residues was determined and used for preparing receptor for docking.

The amino acid residues in 7.5Å of the co-crystallized ligand molecules were used to define the active site. In case of ALR1, the reference ligand was FX4 ([(5*Z*)-5-{[3-(carboxymethoxy)-4-methoxyphenyl]methylidene}-2,4-dioxo-1,3-thiazolidin-3-yl]acetic acid) while in case of ALR2, the reference ligand was IDD594 (2-(2-{[(4-bromo-2-fluorophenyl)methyl]carbamothioyl}-5-fluorophenoxy)acetic acid).

Using default parameters of FlexX docking utility, the docking of the corresponding compound was performed after successfully docking the co-crystallized reference ligands. The top most 30 docking poses of the compound was retained for further assessment. The final putative binding mode of the compound was selected after careful visual and Hyde assessment.[50]

OSIRIS drug properties and toxicity profile

For the synthesized pyrazole–rhodanine hybrids (**9a–n**), toxicity and drugability profile was determined using OSIRIS property explorer[52] that uses Lipinski's rule of five.[64] The property explorer was able to screen the compounds for the presence of any toxic group that can lead to toxicity or poor drug bioavailability. Toxicity profiles such as irritation, mutagenicity, tumorigenic and/or reproductive toxicity were examined for the synthesized series of compounds.

Acknowledgements

H. Andleeb is thankful to the Higher Education Commission of Pakistan for the financial support under Indigenous 5000 Ph.D Fellowship program. The University of Oxford (UK) is gratefully acknowledged for analysis of some of the synthesized compounds.

Notes and references

1 S. Wild, G. Roglic, A. Green, R. Sicree and H. King, *Diabetes Care*, 2004, **27**, 1047–1053.
2 P. Z. Zimmet, K. G. Alberti and J. Shaw, *Nature*, 2001, **414**, 782–787.
3 S. van Dieren, J. W. Beulens, Y. T. van der Schouw, D. E. Grobbee and B. Neal, *Eur. J. Cardiovasc. Prev. Rehabil.*, 2010, **17**, S3–S8.
4 International Diabetes Federation. Diabetes Atlas, 5th edition. (http://www.idf.org/diabetesatlas).
5 S. Sartini, S. Cosconati, L. Marinelli, E. Barresi, S. Di Maro, F. Simorini, S. Taliani, S. Salerno, A. M. Marini, F. Da Settimo, E. Novellino and C. La Motta, *J. Med. Chem.*, 2012, **55**(23), 10523-10531.
6 S. M. Grundy, I. J Benjamin, G. L. Burke, A. Chait, R. H. Eckel, B. V. Howard, W. Mitch, S. C., Jr. Smith, J. R. Sowers, *Circulation* 1999, **100**, 1134–1146.
7 P. Fresneau, M. Cussac, J.-M. Morand, B. Szymonski, D. Tranqui and G. Leclerc, *J. Med. Chem.*, 1998, **41**(24), 4706–4715.
8 J. H. Kinoshita, L. O. Merola, K. Satoh and E. Dikmak, *Nature*, 1962, **194**, 1085–1087.
9 W. G. Jr. Robison, P. F. Kador and J. H. Kinoshita, *Science,* 1983, **221**, 1177–1179.
10 D. R. Tomlinson, G. B. Willars and A. L. Carrington, *Pharmacol. Ther.*, 1992, **54**(2), 151–194.
11 P. F. Kador, J. H. Kinoshita and N. E. Sharpless, *J. Med. Chem.*, 1985, **28**, 841–849.
12 L. G. Humber, *Prog. Med. Chem.*, 1987, **24**, 299–343.
13 Kador, P. F. *Med. Res. Rev.*, 1988, **8**(3), 325–352.
14 E. R. Larson, C. A. Lipinski and R. Sarges, *Med. Res. Rev.*, 1988, **8**(2), 159–186.
15 X. Qin, X. Hao, H. Han, S. Zhu, Y. Yang, B. Wu, S. Hussain, S. Parveen, C. Jing, B. Ma and C. Zhu, *J. Med. Chem.*, 2015, **58**(3), 1254–1267.
16 M. Brownlee, *Nature*, 2001, **414**, 813–820.
17 F. W. Newell, Ophthalmology: Principles and Concepts, 5th Edition. London: The CV Mosby Company, 1982, pp. 332.
18 V. J. Demopoulos, *Curr. Med. Chem.*, 2009, **6**, 734–752.
19 K. V. Ramana and S. K. Srivastava, *Int. J. Biochem. Cell Biol.* 2010, **1**, 17–20.
20 Ramana, K. V. *Biomol. Concepts* 2011, **1–2**, 103–114.
21 Y. Iwata, M. Arisawa, R. Hamada, Y. Kita, M. Y. Mizutani, N. Tomioka, A. Itai and S. Miyamoto, *J. Med. Chem.*, 2001, **11**, 1718–1728.
22 S. Taketomi, T. Fujita and K. Yokono, *Diabetes. Res. Clin. Pr.*, 1988, **5**(2), 125–134.
23 M. K. Cavaghan, D. A. Ehrmann, M. M. Byrne, and K. S. Polonsky, *J. Clin. Invest.* 1997, **100(3)**, 530–537.
24 R. Kawamori, T. Kadowaki, M. Onji and Y. Seino, *Diabetes. Res. Clin. Pr.*, 2007, **76**(2), 229–235.
25 J. Chilcott, P. Tappenden, M. L. Jones and J. P. Wight, *Clin. Ther.*, 2001, **23**(11), 1792–1823.
26 S. Kahn, S. Haffner, M. Heise, W. Herman, R. Holman, N. Jones, B. Kravitz, J. Lachin, M. O'Neill, B. Zinman and G. Viberti, *N. Engl. J. Med.*, 2006, **355**(23), 2427–2443.
27 T. Kawai, I. Takei, M. Tokui, O. Funae, K. Miyamoto, M. Tabata, T. Hirata, T. Saruta, A. Shimada and H. Itoh, *J. Diabetes. Complicat.*, 2010, **24**(6), 424–432.
28 T. Ikeda, K. Iwata and Y. Tanaka, *Diabetes. Res. Clin. Pr.*, 1999, **43**(3), 193–198.
29 K. E. Schemmel, R. S. Padiyara and J. J. D'Souza, *J. Diabetes. Complicat.*, 2010, **5**, 354–360.
30 S. Manfredini, R. Bazzanini, P. G. Baraldi, M. Guarneri, D. Simoni, M. E. Marongiu, A. Pani, E. Tramontano and C. P. La, *J. Med. Chem.*, 1992, **35**, 917–924.
31 S. Manfredini, R. Bazzanini, P. G. Baraldi, M. Bonora, M, Marangoni, D. Simoni, A. Pani, F. Scintu, E. Pinna, L. Pisano and C. P. La, *Anti-Cancer Drug Des.*, 1996, **11**, 193–204.
32 H. J. Park, K. Lee, S. J. Park, B. Ahn, J. C. Lee, H. Cho and K. I. Lee, *Bioorg. Med. Chem. Lett.*, 2005, **15**, 3307–3312.
33 T. D. Penning, J. J. Talley, S. R. Bertenshaw, J. S. Carter, P. W. Collins, S. Docter, M. J. Graneto, L. F. Lee, J. W. Malecha, J. M. Miyashiro, R. S. Rogers, D. J. Rogier, S. S. Yu, G. D.

View Article Online
DOI: 10.1039/C6RA14531K

Anderson, E. G. Burton, J. N. Cogburn, S. A. Gregory, C. M. Koboldt, W. E. Perkins, K. Seibert, A. W. Veenhuizen, Y. Y. Zhang and P. C. Isakson, *J. Med. Chem*., 1997, **40**, 1347–1365.

34 K. L. Kees, J. J. Fitzgerald, K. E. Steiner, J. F. Mattes, B. Mihan, T. Tosi, D. Mondoro and M. L. McCaleb, *J. Med. Chem*., 1996, **39**, 3920–3928.

35 G. R. Bebernitz, G. Argentieri, B. Battle, C. Brennan, B. Balkan, B. F. Burkey, M. Eckhardt, J. Gao, P. Kapa, R. J. Strohschein, H. F. Schuster, M. Wilson and D. D. Xu, *J. Med. Chem*., 2001, **44**, 2601–2611.

36 B. Cottineau, P. Toto, C. Marot, A. Pipaud, J. Chenault, *Bioorg. Med. Chem. Lett.* 2002, **12**(16), 2105-2108.

37 T. Biftu, R. Sinha-Roy, P. Chen, X. Qian, D. Feng, J. T. Kuethe, G. Scapin, Y. D. Gao, Y. Yan, D. Krueger, A. Bak, G. Eiermann, J. He, J. Cox, J. Hicks, K. Lyons, H. He, G. Salituro, S. Tong, S. Patel, G. Doss, A. Petrov, J. Wu, S. S. Xu, C. Sewall, X. Zhang, B. Zhang, N. A. Thornberry and A. E. Weber, *J. Med. Chem.*, 2014, **57**(8), 3205–3212.

38 K. D. Freeman-Cook, P. Amor, S. Bader, L. M. Buzon, S. B. Coffey, J. W. Corbett, K. J. Dirico, S. D. Doran, R. L. Elliott, W. Esler, A. Guzman-Perez, K. E. Henegar, J. A. Houser, C. S. Jones, C. Limberakis, K. Loomis, K. McPherson, S. Murdande, K. L. Nelson, D. Phillion, B. S. Pierce, W. Song, E. Sugarman, S. Tapley, M. Tu and Z. Zhao, *J. Med. Chem.*, 2012, **55**(2), 935–942.

39 K. L. Kees, J. J. Fitzgerald, K. E. Steiner, J. F. Mattes, B. Mihan, T. Tosi, D. Mondoro and M. L. McCaleb, *J. Med. Chem.*, 1996, **39**(20), 3920–3928.

40 R. J. Patch, L. L. Searle, A. J. Kim, D. De, X. Zhu, H. B. Askari, J. C. O'Neill, M. C. Abad, D. Rentzeperis, J. Liu, M. Kemmerer, L. Lin, J. Kasturi, J. G. Geisler, J. M. Lenhard, M. R. Player and M. D. Gaul, *J. Med. Chem.*, 2011, **54**(3), 788–808.

41 J. R. Shroff, V. Bandurco, R. Desai, S. Kobrin and P. Cervoni, *J. Med. Chem.*, 1981, **24**(12), 1521–1525.

42 a) Z. Iqbal, S. Ali, J. Iqbal, Q. Abbas, I. Z. Qureshi and S. Hameed, *Bioorg. Med. Chem. Lett*., 2013, **23**, 488–491. b) Z. Iqbal, S. Hameed, S. Ali, Y. Tehseen, M. Shahid and J. Iqbal, *Eur. J. Med. Chem.,* 2015, **98**, 127–138.

43 (a) V. Ramesh, B. A. Rao, P. Sharma, B. Swarna, D. Thummuri, K. Srinivas, V. G. M. Naidu and V. J. Rao, *Eur. J. Med. Chem*., 2014, **83**, 569–580; For related procedures for the synthesis of rhodanine compounds, see: (b) H. Fu, X. Hou, L. Wang, Y. Dun, X. Yang and H. Fang, *Bioorg. Med. Chem. Lett*., 2015, **25**, 5265–5269; (c) L.-F. Yu, Y.-Y. Li, M.-B. Su, M. Zhang, W. Zhang, L.-N. Zhang, T. Pang, R.-T. Zhang, B. Liu, J.-Y. Li, J. Li and F.-J. Nan, *ACS Med. Chem. Lett*., 2013, **4**, 475–480. (d) K. Toubal, A. Djafri, A. Chouaih, and A. Talbi, Molecules. 2012, 17, 3501-3509

44 S. Bansal, M. Bala , S. K. Suthar, S. Choudhary, S. Bhattacharya, V. Bhardwaj , S. Singla and A. Joseph, *Eur. J. Med. Chem.,* 2014, **80**, 167-174.

45 (a). P. Mandal, Mithuna, A. Garg, S. S. Sahetya, S. R. Nagendra, H. S. Sripad, M. M. Manjunath, Sitaram, Mukesh Soni, R. N. Baig, S. V. Kumarc and B. R. P. Kumar *RSC Adv*., 2016, **6**, 58641-58653; (b) W. T. Sing, C. L. Lee, S. L. Yeo, S. P. Lim, M. M. Sim, *Bioorg. Med. Chem. Lett*., 2001, **11**, 91–94; (c) A. I. Khodair, *J. Heterocyc. Chem*., 2002, **39**, 1153–1160; (d) Y. Ohishi, T. Mukai, M. Nagahara, M. Yajima, N. Kajikawa, K. Miahara, T. Takano, *Chem. Pharm. Bull*., 1990, **38**, 1911–1919; (e) J. C. Richerd and R. Clark, *Can. J. Cherm*., 1964, **42**, 2073.

46 O. A. Barski, S. M. Tipparaju and A. Bhatnagar, *Drug Metab. Rev.*, 2008, **40**(4), 553–624.

47 (a) D. Rakowitz, R. Maccari, R. Ottana and M. G. Vigorita, *Bioorg. Med. Chem*., 2006, **14**, 567–574; (b) S. Ali, A. Saeed, N. Abbas, M. Shahid, M. Bolte and J. Iqbal, *Med. Chem. Commun*., 2012, **3**, 1428–1434.

48 LeadIT, 2.1.8; BioSolveIT GmbH, Germany, **2014**.

49 O. El-Kabbani, V. Carbone, C. Darmanin, M. Oka, A. Mitschler, A. Podjarny, C. Schulze-Briese and R. P.-T. Chung, *J. Med. Chem*., 2005, **48**(17), 5536–5542.

50 N. Schneider, G. Lange, S. Hindle, R. Klein and M. Rarey, *J. Comput. Aided Mol. Des.*, 2013, **27**(1), 15–29.

51 O. El-Kabbani, C. Darmanin, T. R. Schneider, I. Hazemann, F. Ruiz, M. Oka, A. Joachimiak, C. Schulze-Briese, T. Tomizaki and A. Mitschler, *Proteins*, 2004, **55**(4), 805–813.

52 T. Sander, OSIRIS property explorer. Allschwil: Actelion Pharmaceuticals Ltd 2001. http://www.organic-chemistry.org/prog/peo/index.html.

53 C. Nitsche and C. D. Klein, *Tetrahedron Lett*., 2012, **53**, 5197–5201.

54 X.-Y. He, P. Zou, J. Qiu, L. Hou, S. Jiang, S. Liu and L. Xie, *Bioorg. Med. Chem*., 2011, **19**, 6726–6734.

55 N. Paul and S. Muthusubramanian, *Helv. Chim. Acta*, 2013, **96**, 452–457.

56 O. Prakash, K. Pannu and A. Kumar, *Molecules*, 2006, **11**, 43–48.

57 N. C. Desai, V. V. Joshi, K. M. Rajpara, H. V. Vaghani and H. M. Satodiya, *J. Fluorine Chem*., 2012, **142**, 67–78.

58 S. G. Alegaon, M. B. Hirpara, K. R. Alagawadi, K. K. Hullatti and K. Kashniyal, *Bioorg. Med. Chem. Lett*., 2014, **24**, 5324–5329.

59 I. Ali, A. Haque, K. Saleem and M. F. Hsieh, *Bioorg. Med. Chem*., 2013, **21**, 3808–3820.

60 A. Saeed, Y. Tehseen, H. Rafique, N. J. Furtmann, U. Flörke, J. Iqbal, *Med. Chem. Comm*., 2014, **5**(9), 1371–1380.

61 ACD/ChemSketch. Advanced Chemistry Development, Inc.: Toronto, ON, Canada, 2014.

62 H. M. Berman, J. Westbrook, Z. Feng, G. Gilliland, T. Bhat, H. Weissig, I. N. Shindyalov and P. E. Bourne, *Nucleic Acids Res*., 2000, **28**(1), 235–242.

63 S. Bietz, S. Urbaczek, B. Schulz and M. Rarey, *J. ChemInform.*, 2014, **6**, 12.

64 C. A. Lipinski, F. Lombardo, B. W. Dominy and P. J. Feeney, *Adv. Drug Deliv. Rev*., 2012, **64**, 4–17.

View Article Online
DOI: 10.1039/C6RA14531K

Identification of novel pyrazole–rhodanine hybrid scaffolds as potent inhibitors of aldose reductase: design, synthesis, biological evaluation and molecular docking analysis

Hina Andleeb,[a] Yildiz Tehseen,[b] Syed Jawad Ali Shah,[b] Imtiaz Khan,[a] Jamshed Iqbal[b]*and Shahid Hameed[a]*

For TOC use only:

A series of novel pyrazole-rhodanine derivatives was designed, synthesized, and biologically evaluated for their potential inhibitory effect on both aldehyde reductase (ALR1) and aldose reductase (ALR2).

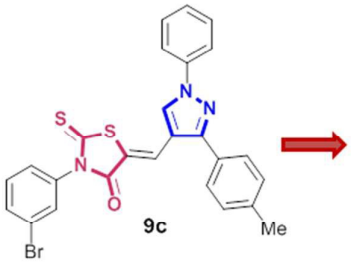

13 more examples

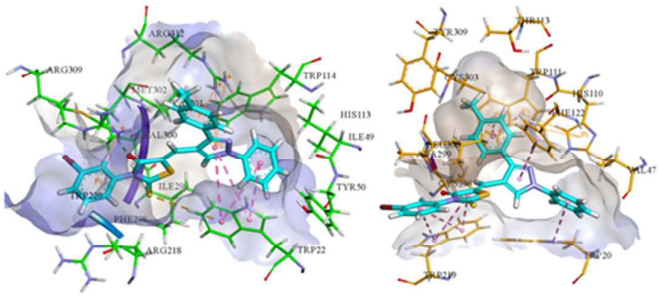

Putative binding mode of inhibitor **9c** inside the active pocket of ALR1 and ALR2